Supplement of Nat. Hazards Earth Syst. Sci., 25, 1169–1185, 2025
https://doi.org/10.5194/nhess-25-1169-2025-supplement

Natural Hazards and Earth System Sciences
Open Access

Supplement of

Tsunami detection methods for ocean-bottom pressure gauges

Cesare Angeli et al.

Correspondence to: Cesare Angeli (cesare.angeli2@unibo.it)

S1 - Sensitivity of TDA to data availability

Detection curves for TDA presented for the background analysis examples in section 3.1, especially cases A to E, represent ideal cases. In each case, we computed tidal coefficients using differing amount of data and we kept the best fitting set of coefficients. As a rule of thumb, we found that 7 to 9 months of previous data give the best performing detection curves.

To show this, the coefficients for the harmonic tidal model have been computed from time series ending two weeks before the starting point of the case (Tab. 1 in the main text) and starting at different times before that. The result are shown in Fig. S1. For each case, the maximum, minimum and mean value of each detection curve is plotted. It is immediately evident that detection curves amplitude is strongly dependent on how many data we use to compute the tidal model. In particular, the amplitude tends to stabilize within $\pm 2\,\mathrm{cm}$ when at least 6 to 7 months of data are used. Fewer data not only result in larger oscillations, but also in more asymmetric distributions, as we can see from the signal averages, i.e. the red curves, in Fig. S1. We point out a few factors. The first is that it is difficult to have both a symmetric distribution and the average as close to zero as possible. In fact, in cases B, C, and E, the amount of data needed to obtain the narrower distributions are not the ones with the closest to zero average. We recall that an asymmetric distribution would lead to the detectability of weak tsunamis to depend on their polarity. On the other hand, a broader distribution would give us a technique that is less capable of detecting weak tsunamis in general. The second factor to note in Fig. S1 is that, while the variability ranges initially converges around zero, there may be cases where this trend breaks for large enough time series. In case A, we can notice that, after reaching a narrow and symmetrical distribution for around 8 months of data, then both the minimum and maximum of the detection curves increase with longer time series. In case C, we can appreciate a signifcant jump for time series length greater than 12 months. These effects may be related to the possible presence of very long term trends in OBPG records, which, if not taken into account, make tidal coeffcients computation dependent on which sections of the time series we use.

As a rule of thumb, to have background detection curves within 2 to 3 cm, we can simply propose the rule of thumb of using 7 to 9 months of previous data to compute tidal coeffcients. Accordingly, tidal coefficients for the example with simultaneous signals have been computed using 7 months of previous data, ending one week before the beginning of the time series.

S2 - Listings for Matlab codes for EOF and TDA

Matlab code for the creation of the EOF basis matrix:

```
%%%%%%%%%%%%%%%%%%%%%%%%%%%%%%%%%%%%%%
%% EOF DETECTION - BASIS EXTRACTION %%
%%%%%%%%%%%%%%%%%%%%%%%%%%%%%%%%%%%%%%

%% File reading
% the scripts assumes the files in the NetCDF format as
% in the NDBC's Unassessed Ocean Pressure Data dataset
```

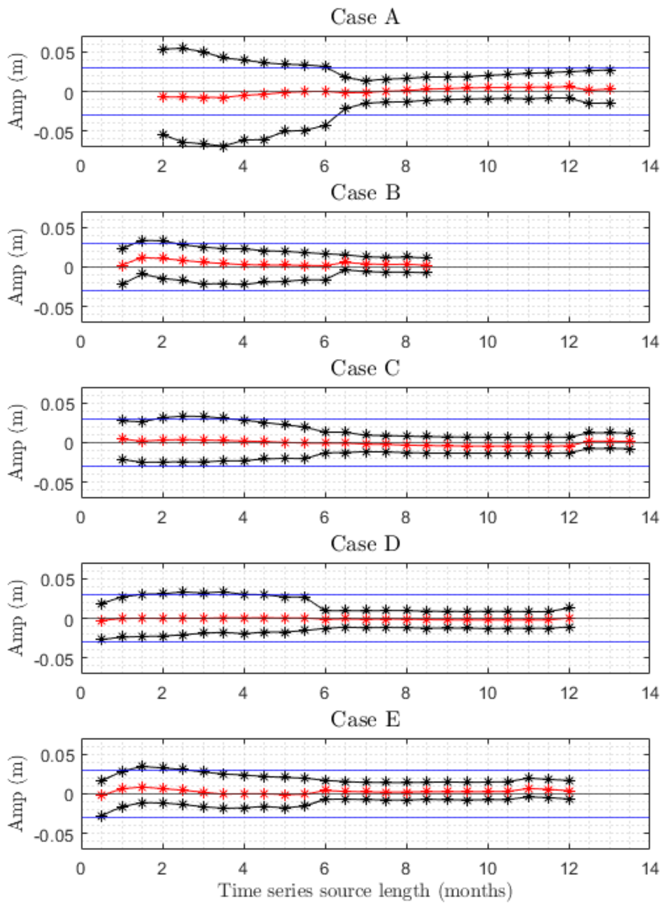

Fig. S1: Variability range of TDA detection curves for different tidal models. For each case, we plot the maximum and minimum (in black) and the average value (in red) of each detection curve corresponding to a different length of source data used to compute tidal coefficients. Horizontal blue lines corresponds to amplitudes of ±3 cm. The smallest data length for which data are plotted in each case is the smallest for which UTide converges. The largest data length used correspond to the maximum amount of data available in that deployment.

```
file = 'pat/to/raw/dart/data.nc';
time      = ncread(file , "time");
pressure = ncread(file , "seafloor_pressure_abs_raw");

last = 8122790   % to manually remove the first and last portion of
first = 1300     % data. Choose depending on the specific time series.

time = time(first:last);
pressure = pressure(first:last);

%% Basis creation

M = 99*60;      % segment length
N = 150;     % number of segments
n = 7;       % components to keep

seg = randi(length(time)-(N+1)*M, N, 1)+M;
seg = sort(seg);
for i = 1:length(seg)
    seg(i) = seg(i)+(M)*(i-1);
end

zeta = [];
for i = 1:length(seg)
    segmento = pressure(seg(i):seg(i)+M-1) - mean(pressure(seg(i):seg(i)+M-1));
    zeta = [zeta segmento];
end

C = zeta*zeta';
Cb = C + flip(flip(C), 2);
[V, D] = eigs(Cb, n);
ff = V*V';                       % Result! Tides can be extracted from signal s
                                 % by computing ff*s
```

Matlab code for the application of TDA to detided signals

```
%% file reading
% reads a file 'detided_empty.dat' which has 3 columns:
% time, forecast tide, signal - forecast tide
% forecast tide has been computed using UTide (Pawlowicz et al. 2002)

A = readmatrix('detided_empty.dat');
t = A(:, 1);
data = A(:, 3);

%% Fir filter design

dt = 15;                  % acquisition sampling time of DART stations
Fs = 1/dt;
bnd = [1/7200 1/240];  % period band between 4 and 120 minutes.
```

```
ord = 4000;
bp = designfilt('bandpassfir','FilterOrder',ord, ...
    'CutoffFrequency1',bnd(1),'CutoffFrequency2',bnd(2), ...
    'SampleRate',Fs);
c = bp.Coefficients;   % FIR filter coefficients


%%
pred = zeros(length(data), 1); % allocate memory for detection curve

% compute eq. 3 by Chierici et al. 2017
for n = ord/2+2:length(data)
    pred(n) = c(1)*data(n) + 2*dot(c(ord/2+1:end), flip(data(n-ord/2-1:n-1)));
end

%% save detection curves to disk
writematrix([t pred], 'tda_4m.dat', 'Delimiter', ' ')
```

S3 - Plots for background analyses, Cases B, C, D, E

In the following, the plots for cases B, C, D and E in Tab. 1 in the main text, relative to the analysis fo background signals as described in section 3.1. For the analysis fo these plots, we refer to the main body of the paper

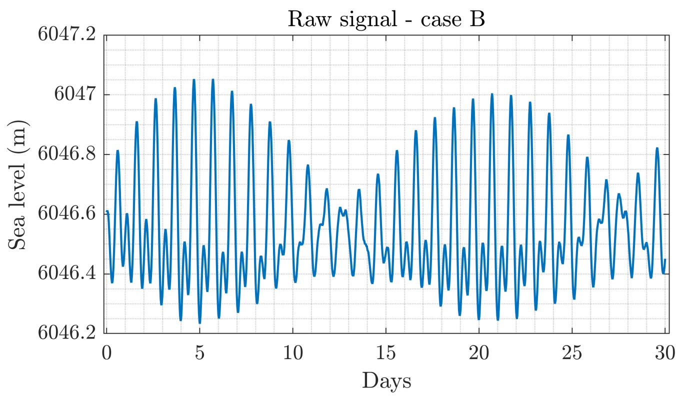

Fig. S2: Raw data from DART 52402 for the month of July 2016.

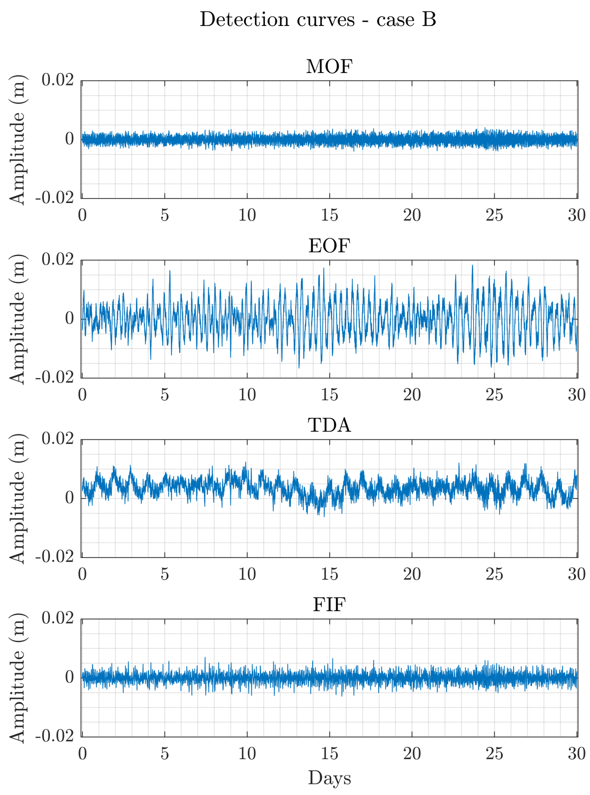

Fig. S3: Detection curves for each detection technique for DART 52402, July 2016 (Fig. S2).

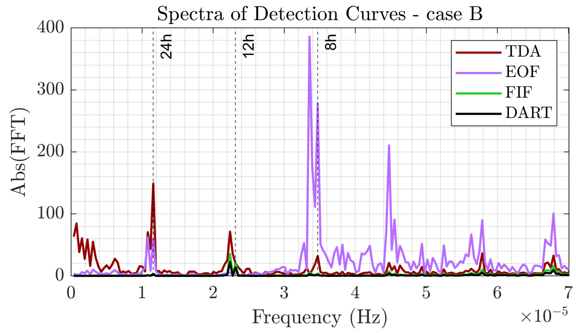

Fig. S4: Detection curves for each detection curve in Fig. S3, relative to data from DART 52402, July 2016 (Fig. S2).

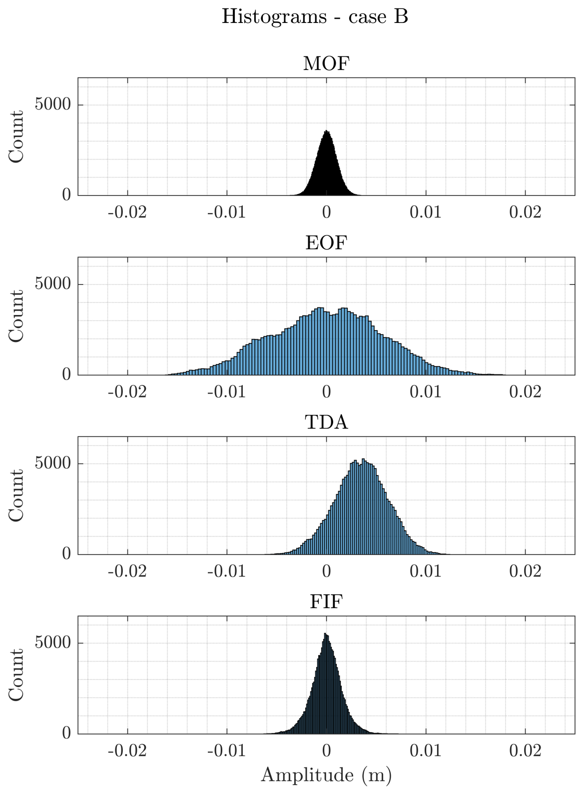

Fig. S5: Histograms of each detection curve in Fig. S3, relative to data from DART 52402, July 2016 (Fig. S2).

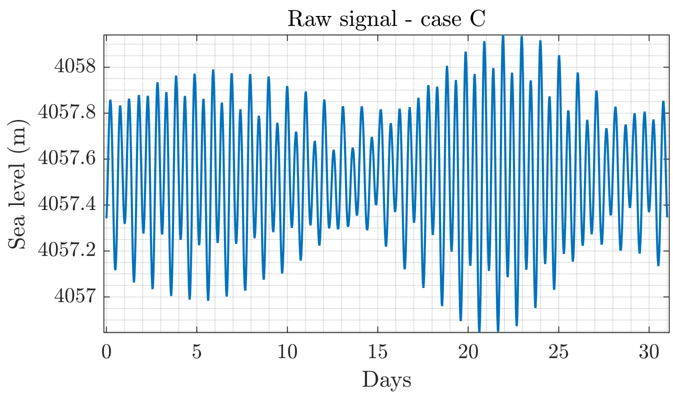

Fig. S6: Raw data from DART 32403 for the month of January 2019.

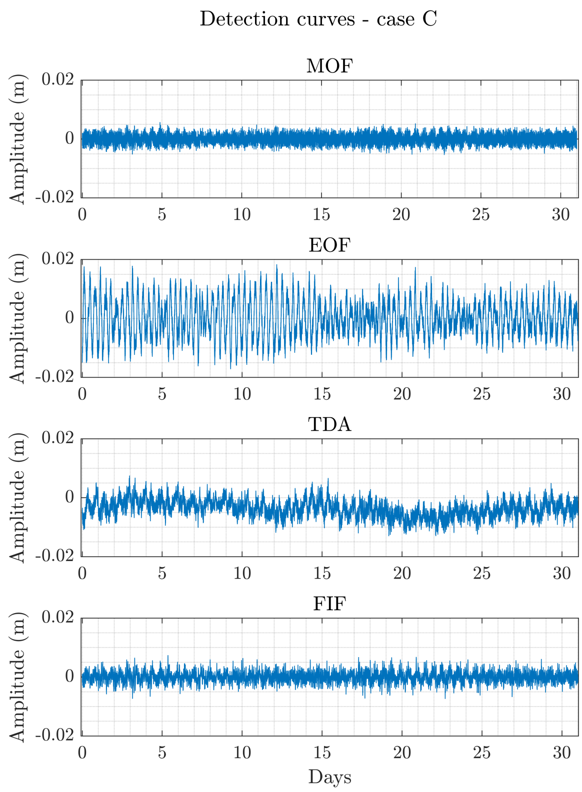

Fig. S7: Detection curves for each detection technique for DART 32403, January 2019 (Fig. S6).

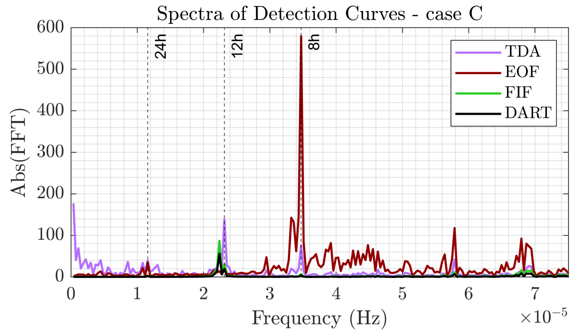

Fig. S8: Detection curves for each detection curve in Fig. S7, relative to data from DART 32403, January 2019 (Fig. S6).

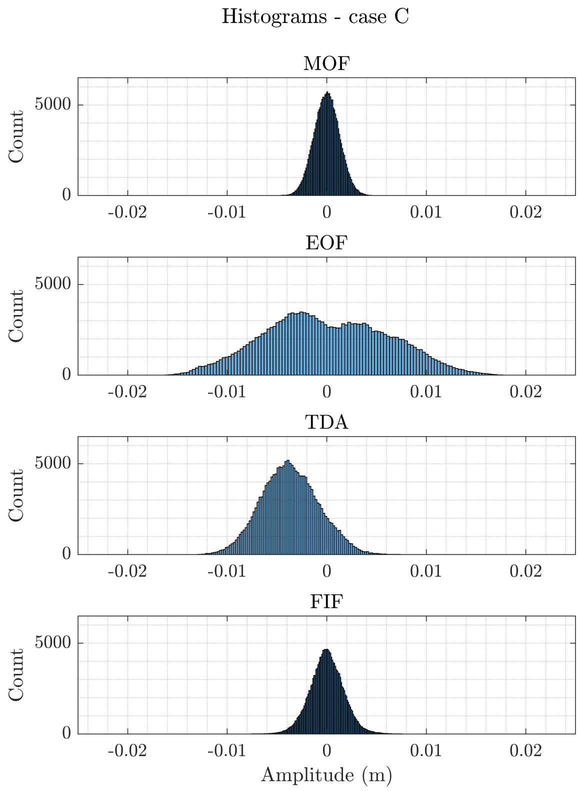

Fig. S9: Histograms of each detection curve in Fig. S7, relative to data from DART 32403, January 2019 (Fig. S6).

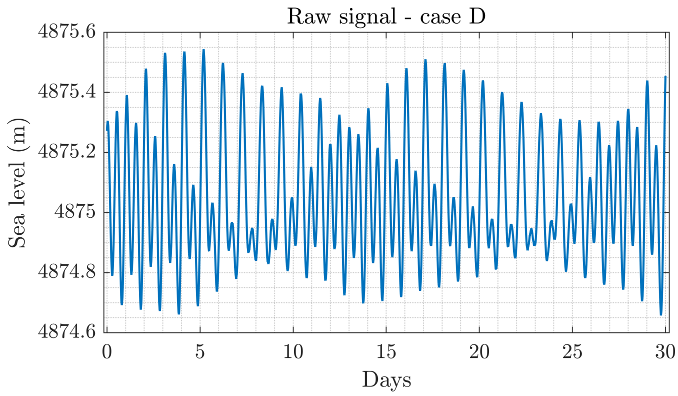

Fig. S10: Raw data from DART 51407 for the month of 15th April to 14th May 2022.

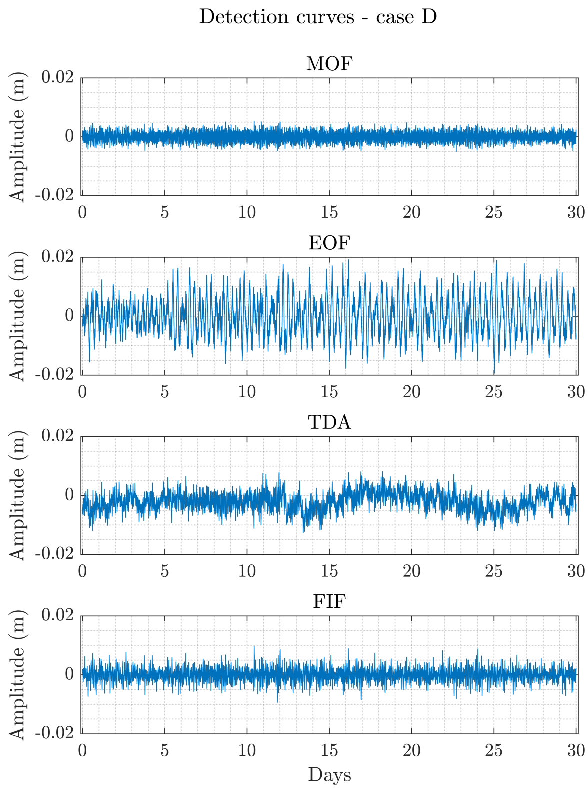

Fig. S11: Detection curves for each detection technique for DART 51407, 15th April to 14th May 2022 (Fig. S10).

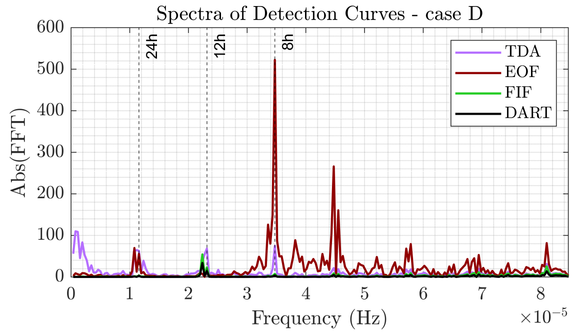

Fig. S12: Detection curves for each detection curve in Fig. S11, relative to data from DART 51407, 15th April to 14th May 2022 (Fig. S10).

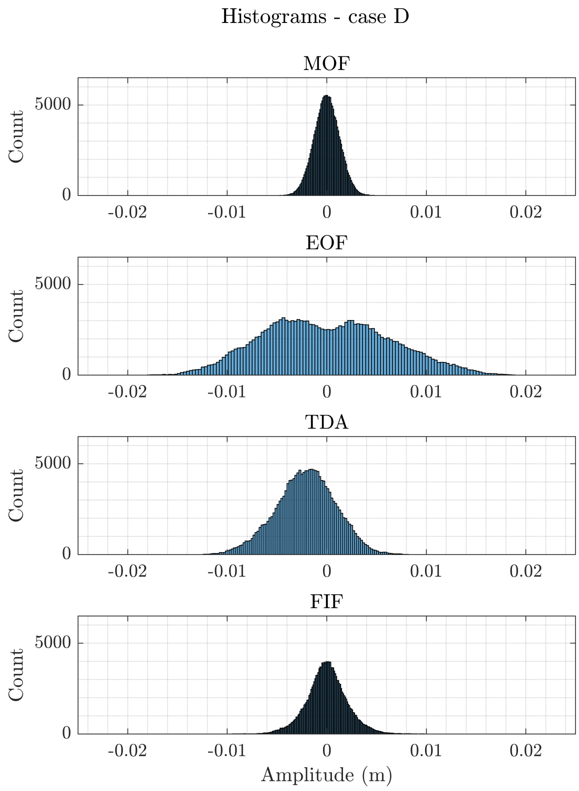

Fig. S13: Histograms of each detection curve in Fig. S11, relative to data from DART 51407, 15th April to 14th May 2022 (Fig. S10).

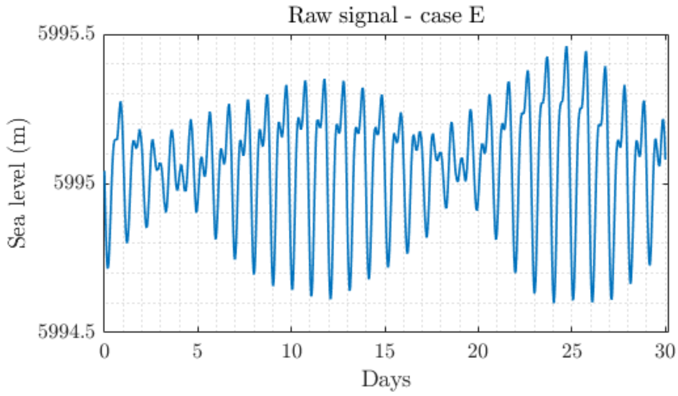

Fig. S14: Raw data from DART 21413 for the month of June 2021.

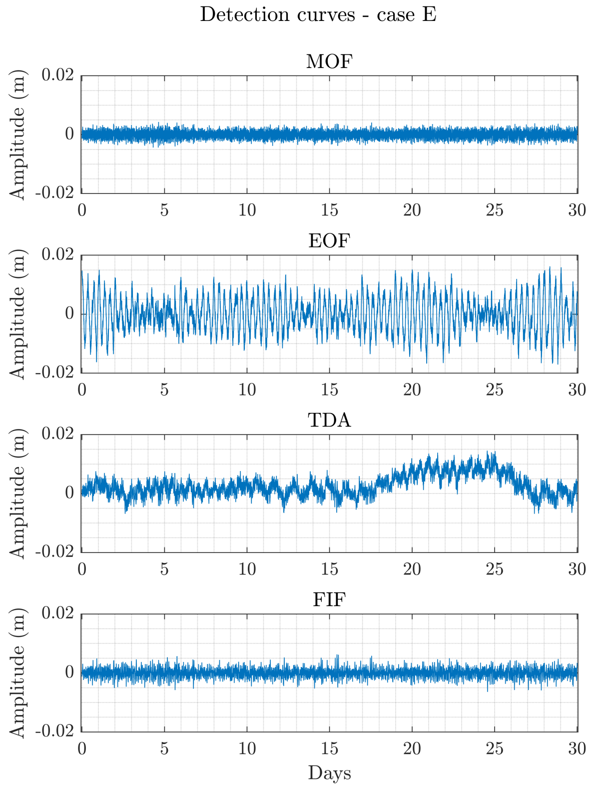

Fig. S15: Detection curves for each detection technique for DART 21413, June 2021 (Fig. S14).

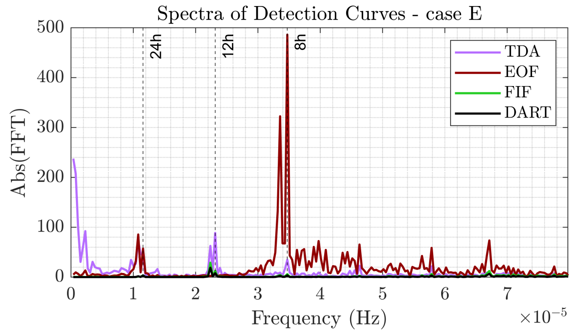

Fig. S16: Detection curves for each detection curve in Fig. S15, relative to data from DART 21413, June 2021 (Fig. S14).

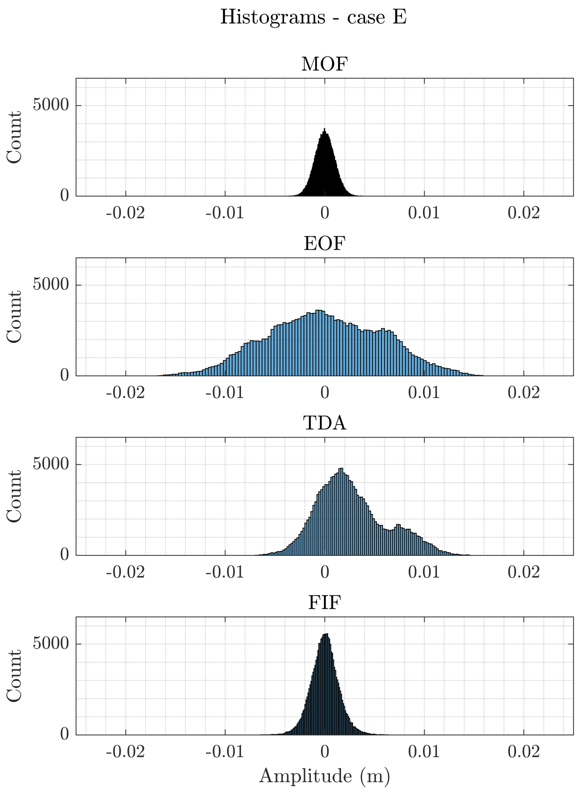

Fig. S17: Histograms of each detection curve in Fig. S15, relative to data from DART 21413, June 2021 (Fig. S14).